Lymph node follicle formation and vaccination responses reconstituted *in vitro* in a human Organ Chip

Girija Goyal[1], Bruce Bausk[1,2], Pranav Prabhala[1], Liangxia Xie[1,2], Danielle Curran[1], Jaclyn Long[1], Limor Cohen[1,2], Oren Levy[1], Rachelle Prantil-Baun[1], David R. Walt[1,2] and Donald E. Ingber[1,3,4*]

[1]Wyss Institute for Biologically Inspired Engineering at Harvard University, Boston, MA 02115, USA; [2]Department of Pathology, Brigham and Women's Hospital, Harvard Medical School, Boston, MA 02115, USA; [3]Vascular Biology Program and Department of Surgery, Boston Children's Hospital and Harvard Medical School, Boston, MA 02115, USA; [4]Harvard John A. Paulson School of Engineering and Applied Sciences, Harvard University, Cambridge, MA 02139, USA.

[*]Corresponding Author: Donald E. Ingber, M.D., Ph.D., Wyss Institute at Harvard University, CLSB5, 3 Blackfan Circle, Boston, MA 02115 (Em: don.ingber@wyss.harvard.edu; Ph: 617-432-7044; Fx: 617-432-7828)

ABSTRACT

Candidate vaccines and immunotherapeutic drugs often fail in clinical trials as human lymph node (LN) physiology is not faithfully modeled in animal models or immune cell cultures. Here we describe a microfluidic Organ Chip culture device that supports self-assembly of human blood-derived B and T lymphocytes into three-dimensional (3D), germinal center-like lymphoid follicles (LFs) containing Activation-Induced Cytidine Deaminase (AID) expressing lymphocytes. These microengineered LFs support plasma cell differentiation upon activation with IL-4 and CD40 agonistic antibody

(AB) or inactivated *S. aureus* Cowan I (SAC). Immunization of the human LN chip with a quadrivalent split virion influenza vaccine resulted in plasma cell formation, viral strain-specific anti-hemagglutinin immunoglobulin G (IgG) production, and a secreted cytokine profile that recapitulates serum responses of vaccinated humans. Thus, the human LN chip may provide a new tool to study human immune reactions, evaluate vaccine responses, and validate the efficacies and toxicities of immunotherapies *in vitro*.

INTRODUCTION

New vaccines and immunotherapies are evaluated in animal models, which can lead to unpredicted toxicities or poor efficacy in clinical trials because of species-specific differences in immune responses (*1*). Preclinical experiments are also conducted *in vitro*, using human immune cells collected from blood; however, even these results can fail in predicting responses in human patients (*2*, *3*). One major reason for this failure is that *in vivo* immune responses commonly occur within the highly specialized microenvironment of the LN that has unique niches, including LFs within its cortex. DNA modifying enzymes required by B cells to switch from one Ab isotype to another, such as AID, are only expressed by B cells resident within the LN (*4*). Upon immune activation by antigen, helper T cells in the LF enable the B cells to switch isotypes and produce high affinity Abs; when activated, LFs are called germinal centers. Class switching is defective in mice or patients lacking functional LNs, leading to recurrent infections and morbidity despite preserved *in vitro* lymphocyte functionality (*5*, *6*). Strong antigens induce extrafollicular Ab production, but this can be limited to IgM, with short lived plasma cells, and poor memory responses. Affinity maturation by somatic hypermutation also only occurs in the germinal center (*7*, *8*).

To accurately predict the safety and efficacy of vaccines, it is therefore necessary to study class switching, plasma cell differentiation, and Ab production within a human LN microenvironment

that recapitulates physiologically relevant LF structure and function. Others have studied cultured human tonsillar lymphocytes obtained from patients (*9*, *10*) or created putative 3D models of the LN (*11*, *12*), but these experimental systems do not demonstrate LN-like biomarkers, *de novo* LF formation or survival of plasma cells. Here, we describe how Organ Chip microfluidic culture technology, which has been successfully used to recapitulate both normal physiology and disease states in multiple other human organs (e.g., lung, intestine, kidney, bone marrow, brain, etc.) (*13–19*), can be applied in combination with human blood-derived lymphocytes to create a functional LN model. This human LN chip exhibits spontaneous LF formation, induction of class switching, and plasma cell development in response to bacterial stimuli, antigen-specific Abs, as well as physiologically relevant human vaccination responses to a commercial influenza vaccine.

RESULTS

Perfusion-induced assembly of T and B lymphocytes into LFs on-chip

We used a microfluidic Organ Chip device composed of two channels separated by a porous membrane (*19*) in which human T and B lymphocytes isolated from apheresis collars were cultured within a gel composed of Matrigel and type I collagen at a high density (1.5-2 x 10^8 cells/ml; 1:1 ratio) in the lower channel while being supplied with oxygen and nutrients through continuous perfusion of culture medium through the upper channel (**Fig. 1A; Supplementary Fig. 1A)**. This cell density was utilized because high density lymphocyte suspension cultures have been shown to be more predictive of clinical responses than lower density cultures (*20*). In contrast to past studies where only small cell aggregates were observed (*21*), the unstimulated T and B lymphocytes self-assembled into larger LFs along the entire length of the channel after 3-4 days of culture on-chip (**Fig. 1B**, **Supplementary Fig. 1B)**, which contained both T and B cells that stained positively for CTLA-4 (**Supplementary Fig. 1C)**.

The T and B cells were found to be in close contact within the follicles, forming cell synapses on-chip (**Supplementary Fig. 1C)**, with polarized expression of the T cell co-receptor CD3 (**Fig. 1C)**. Culture of lymphocytes on ECM coated plates has been shown to induce a similar tissue-like polarization in circulating T cells (*20*, *22*). However, we found T cell polarization to be significantly increased in the Organ Chip cultures containing cells in 3D ECM gels whether maintained under static or perfused conditions compared to cells on planar 2D culture (**Fig. 1C)**. Interestingly, dynamic perfusion of the LN Chip resulted in realignment of fibrils within the ECM gel relative to static gels (**Fig. 1D)**, which was accompanied by a significant increase in the number and size of the follicles compared to static 3D ECM gel cultures after 3 days of perfusion (**Fig. 1D,E; Supplementary Fig. 1E)**. LF formation in static 3D cultures was only observed in ~ 25% (1/4) of the human donors, whereas 100% (6/6) of the perfused LN Chip cultures formed LFs that were also significantly larger in volume (**Fig. 1E).** LF formation requires the chemokine CXCL13 in murine models (*23*) and CXCL13 plasma levels have been correlated with follicle formation and vaccine responses in humans (*24*, *25*). We similarly found that CXCL13 is expressed over 4 to 8 days of culture under baseline conditions, and that exposure of the LN Chip to the bacterial stimulant SAC significantly increased CXCL13 expression at day 8 (**Fig. 1F)**. The total number of LFs decreased by 7 days of culture in the absence of antigenic activation (**Supplementary Fig. 1D)**.

B cell activation and AID expression

B cells in the blood are a minor population compared to T lymphocytes and they are composed largely of naïve B cells characterized as IgD+ CD27- cells. On the other hand, tonsils that contain multiple LFs have a high number of B cells, only about half of which are IgD+ (*26*, *27*) (**Fig. 2A)**. Auto-activation of B cells in high density cultures has been reported previously (*28*) and we observed a similar response: isolated B cells increased their expression of CD27 and

production of both IgM and IgG under static 3D culture conditions (**Supplementary Fig. 2A,B)**. In contrast, B cells cultured at high density in the perfused LN chip under baseline unstimulated conditions remained naïve, as indicated by a high frequency of IgD+ CD27- cells that was similar to isolated PBMCs and significantly higher than that of naïve B cells in tonsils (**Fig. 2A)**. Further, the naïve B cells on-chip only produced IgM (**Supplementary Fig. 2B)**.

The critical Ab class switching response that shifts IgM to IgG production occurs in the LN *in vivo*. This process results from the action of enzymes, such as AID, that are specifically expressed in LN-resident B cells (*4*). Importantly, we detected AID expression in B cells that appeared within LFs as well as in some single cells within the LN Chip using immunofluorescence confocal microscopy (**Fig. 2B; Supplementary Fig. 3A)**. When we quantified the number of AID+ B cells within LFs, we found that AID expression increased linearly with follicle size until the aggregates reached about 120 um^2 in projected area (**Fig. 2C)** but saturated thereafter (**Supplementary Fig. 3B)**. The perfused LN Chips also exhibited greater total AID expression as they promoted more LF formation compared to static cultures (**Supplementary Fig. 3C)**.

Class switching and plasma cell differentiation

Naïve CD27- B cells isolated from apheresis collars using CD27 depletion (**Supplementary Fig. 4**) were combined with T cells, integrated into LN Chips, and stimulated with IL4 and anti-CD40 Ab, which have been previously shown to induce class switching. IgG was detected in the effluents of the LN Chips stimulated with IL4 and anti-CD40 Ab (**Fig. 3A)**, confirming that B cells undergo class switching *in vitro* under these conditions. Moreover, formation of CD138+ plasma cells was detected in a large number of follicles by day 7 in the stimulated LN Chips (**Fig. 3B)**. While CD138 expression could be detected in some single cells, they preferentially co-localized with clustered cells in the self-assembled LFs (**Fig. 3C)**. As bacteria drain to the LNs near

regions of infection, we also used SAC antigen to mimic the presence of dead bacteria in the LN Chip. Exposure to SAC similarly induced plasma cell formation (**Fig. 3D)**, which again was preferentially located within the LFs (**Fig. 3E)**. Importantly, SAC-treated chips also produced robust IgG responses (**Fig. 3F)**. Thus, the LN Chip is able to undergo class switching, form plasma cells, and generate polyclonal IgG Abs in response to a bacterial antigens *in vitro*.

LN Chip recapitulates the human response to influenza vaccination in vitro

Protective immunity requires plasma cell production of antigen-specific Abs. To explore whether we could generate a physiologically relevant vaccination response *in vitro*, we tested the widely used, split virus quadrivalent influenza vaccine, Fluzone. As vaccine antigens are presented by dendritic cells (DC) in the draining LN *in vivo*, we differentiated autologous DCs from monocytes and included them in the ECM gel along with B and T cells as 2% of the total population. Human LN chips generated using cells from 8 different donors were vaccinated with the Fluzone. Unfortunately, we found that the sensitivity of plate-based ELISA methods and hemagglutination inhibition assays commonly used to detect anti-influenza hemagglutinin (HA) Abs in human serum, is too low for analysis of chip effluents (**Supplementary Fig. 5A)**. Thus, we modified a high sensitivity digital ELISA assay (*29*) to detect anti-HA Abs that bind to the HA specific for the influenza A virus used in the Fluzone formulation. These studies revealed that all donors produced Abs at detectable levels, however, they were either low- or high-responders when compared to whole tonsil controls (**Fig. 4A)**. Abs were first detectable in the chip effluents about 5 days after immunization and their levels increased significantly over the following week in both the low and high responder groups (**Fig. 4B)**. Plasma cells also were detected in the vaccinated chips made with cells from donors that exhibited levels of Ab production at 5 days after immunization (**Fig. 4C)**, which is the same time when circulating plasma cells can first be detected in the blood of vaccinated individuals (*30*). Also, as expected based on past work showing the importance of antigen-presenting DCs for generation of a vaccination response

(*31*), we found that when DCs were not included in the LN Chips, there as a significant reduction in levels of anti-influenza specific IgG (**Fig. 4D)** and CXCL13 (**Fig. 4E)**. Interestingly, levels of CXCL13 measured on-chip at an early time (5 days post vaccination) were also predictive of anti-influenza Ab responses in the high responder group (**Fig. 4F)**. Finally, when we quantified levels of 5 cytokines that are important for T cell expansion, survival and helper functions (IFN-γ, IL10, IL2, GM-CSF and IL7) within the effluent of the vaccinated LN Chips. When we compared these results to levels measured in the serum of human volunteers vaccinated with influenza vaccines, we confirmed that the human LN Chip exhibited cytokine profiles that were highly similar to those observed in human volunteers *in vivo* (**Fig. 4G)**.

DISCUSSION

Animal models are the gold standard for advancing vaccine candidates and immunotherapeutics. However, the immune systems of animals are significantly different from humans, which has led to unpredicted toxicities or poor efficacy when vaccines and immunotherapies enter clinical trials (*1*). For example, the severe cytokine syndrome that developed in patients enrolled in the phase I clinical trial of the CD28 superagonist TGN1412 was never observed in preclinical animal models (*2*). Similarly, the tuberculosis vaccine MVA85A, which produced high levels of protection in animals, failed to show any protection in ~1400 infants enrolled in human clinical trials (*3*). Regulatory agencies have tried to address these concerns by stressing the inclusion of *in vitro* experiments using immune cells collected from human blood, which recapitulate immunostimulation of lymphocytes, but they are unable to induce T-dependent antibody responses. Importantly, these *in vitro* assays were included in preclinical studies for both MVA85A and TGN1412, and they clearly were not predictive. Humanized mice have been explored as a possible alternative; however, they are severely immunocompromised, require use of human fetal tissues which has ethical implications, and

lack LNs, which causes defects in class switching, affinity maturation and long-lived plasma cell formation (*32*).

In the present study, we show that the human LN Chip provides an *in vitro*, primary, patient-specific model for modeling antigen-induced immunological responses that recapitulates *in vivo*-like LF formation, including coalescence of B and polarized T cells within large multicellular clusters, Ab class switching, and plasma cell development. Thus, this technology effectively describe simulates self-assembly of developing follicles *in vivo*; however, it also enables real-time visualization using high resolution microscopy, as well as longitudinal quantification of cytokines and class switched antibodies. We also show plasma cell formation within the LFs that self-assemble on-chip when challenged with three independent stimuli: IL4 combined with anti-CD40 Ab, SAC, and the clinically relevant Fluzone vaccine. In contrast, current methods for plasma cell culture rely on extensive cytokine stimulation of memory B cells, stromal cell co-culture, and multiple rounds of manual handling (*9*, *33*, *34*), and they still fail to recapitulate these features of LN architecture and function. Tonsil slices can be used to study antibody generation (*9*, *10*), but human tissue biopsies can be difficult to obtain and maintain in culture, and it is not possible to carry out real-time visualization or easily collect effluents over time.

Our results also revealed new mechanistic insights into LF formation as we were able to observe follicle assembly without the addition of any chemical inducer or exogenous stromal or myeloid cells. This finding is consistent with recent studies of tertiary lymphoid organ formation, which suggest that lymphocytes possess all the necessary factors to induce LF formation (*35*, *36*).

We found that lymphocytes were polarized in 3D matrix culture under static and perfused conditions as the CD3 and CTLA-4 proteins could be seen asymmetrically localized, often at the synapse between two cells. Further analysis of this process revealed that LF formation and

ECM fibril reorganization induced by fluid flow occurred concomitantly. Physical forces and ECM reorganization underlie many developmental processes and the microfluidic LN Chip can be used to explore this link between matrix realignment and LF formation in the future. The findings that 3D culture induces AID expression in B cells, and that the number of AID-expressing cells increases as the follicle size increases, are also novel. Further, our results revealed a link between CXCL13 induction and antigenic stimulation of follicle formation, as well as antibody production, by SAC and Fluzone, which may help to explain why serum CXCL13 levels predict vaccine responses in humans (*24*, *25*).

Thus, the human LN chip has advanced our understanding of LF physiology by revealing key environmental parameters that can reprogram blood lymphocytes to organize themselves into LFs, including cell composition, density, fluidic perfusion, and ECM realignment, in addition to the chemokine milieu. In addition, our findings raise the intriguing possibility that dynamic perfusion of LNs or tertiary lymphoid organs may actively promote LF formation and growth, which is consistent with the observation that lymphatic vessel development accompanies tertiary lymphoid organ development (*37*, *38*) and LN formation can be inhibited by suppressing lymphatic vessel formation.

In vitro 3D models of the human LN have been explored in the past, such as the MIMIC system that mixes microbeads bound to T or B cells (*11*), and the HuALN system that uses a continuously perfused mesh as a tissue-like support (*12*). However, neither of these models produce detectable LF formation or robust plasma cell formation, and only modest production of IgG was observed. To our knowledge, the human LN chip is the first study to report self-assembly of 3D LFs and induction of germinal center-like structures expressing AID and CXCL13 in the absence of immunostimulation, and in response to fluidic perfusion alone.

We also observed unequivocal class switching using IL-4 and anti-CD40 Ab stimulation of chips created using naïve B cells mixed with bulk T cells. While these stimuli can induce class switching in 2D cultures of naïve B cells, treatment of human LN chips with IL-4 and anti-CD40 Ab lead to robust expansion of plasma cells that were preferentially localized in LFs, which does not occur in 2D cultures. Furthermore, while strong antigenic stimulation can drive Ab production and even plasma cell formation without requiring a germinal center, extrafollicular reactions are often restricted to IgM production and they do not support affinity maturation (*7*, *8*). We did not investigate somatic hypermutation in this study, as our work was aimed towards generating a tool for preclinical testing of vaccines and immunotherapies; however, this could be explored in the future.

Testing new influenza vaccines and new viral strains is a huge burden on the healthcare system as the vaccines must be repeatedly optimized because recombination between influenza virus strains is very common and influenza surface antigens are highly mutable. Influenza vaccines are currently tested in ferrets and show only 30-60% protection in humans (*39*). Accurate *in vitro* assessment of influenza vaccines and new strains with primary human cells, modeling the generation of plasma cells and class-switched antibodies would therefore be a significant advance, reducing the need to rely on animal models. Importantly, when we tested the utility of the human LN chip by vaccinating chips made from 10 independent donors with Fluzone, we detected donor-specific responses with formation of plasma cells in the more highly responding donors and production of cytokine biomarkers that replicated serum levels measured from vaccinated human volunteers. Thus, these data show that the human lymph node is a valuable preclinical tool that can overcome the limitations of humanized mice and inform clinical trials of vaccines. As we used bulk B and T cells in the human LN chips that were treated with Fluzone, it is possible that the high responders had preexisting memory for the Fluzone antigens. However, we chose this strategy as it replicates the administration of seasonal influenza

vaccines in human patients who have varying degrees of past exposure to the vaccine and closely related cross-reactive viral strains. Finally, the high sensitivity digital anti-HA ELISA described here can complement traditional methods of quantifying anti-influenza antibodies that can predict protection from influenza in seropositive donors. but are severely limited in sensitivity.

In summary, we describe an *in vitro* Organ Chip model of the human LN composed of donor specific primary lymphocytes and DCs that harnesses microfluidics to promote self-assembly of LFs that recapitulate several LN functions. Key improvements as compared to humanized mice and other reported *in vitro* systems including follicle formation, which can be observed over time *in situ* using high resolution imaging, timely induction of plasma cells as seen *in vivo,* Ab class switching, and cytokine production in response to multiple antigens, including a commercial influenza vaccine. The human LN Chip is also patient-specific, and it recapitulates donor variability in Ab responses to vaccination with Fluzone, further demonstrating its value as a preclinical tool to study vaccines and immunotherapeutic drugs in a patient-specific manner and inform future clinical trials.

Methods and Materials

LN Chip Culture

Apheresis collars, a by-product of platelet isolation, were obtained from Brigham and Women's Hospital under the approval obtained from the Institution Review Board at Harvard University. PBMC were isolated by density centrifugation using Lymphoprep (StemCell Technologies, 07801), and magnetic beads were used for negative selection of bulk B cells (StemCell Technologies, 19054) or naïve B cells (17254), T cells (17951) and monocytes (19058). Isolated cells were counted and directly seeded on chip or frozen in Recovery™ Cell Culture Freezing Medium (Gibco, 12648-010). Monocytes were differentiated into DCs as previously described.

Briefly, $1X10^6$ monocytes were cultured in complete RPMI (RPMI 1640, Gibco, 72400-047), 10% Fetal bovine Serum [FBS, Gibco, 10082-147], 1% Penicillin/Streptomycin (Gibco, 15140122) and 400ng/ml GM-CSF (Mitenyi Biotec, 130-095-372) and 250ng/ml IL-4 (130-094-117) for 5-6 days with 50% of the media being replaced with fresh media and cytokines every 2-3 days.

Prior to seeding, chips were treated with 1% 3-Aminopropyltrimethoxysilane (Sigma, 281778) in ethanol for 1 hour and then incubated in an 80°C oven overnight to cross-link the seeded ECM to the surfaces of the channel. Cells were introduced in the bottom channel of 2-channel Organ Chips fabricated as described previously (*19*) or obtained from a vendor (Emulate Inc.) mixed with complete RPMI, Matrigel (60%; Corning, 356234) and type I collagen (15%; Corning, 354249) at a concentration of 1.5-2 X 10^8 cells/ml and the ECM was allowed to gel for 30 minutes in a 37°C cell culture incubator. The top channel of the chip was filled with media and channel entry and exit ports were plugged with 200ul tips containing media. The following day chips were perfused using peristaltic pumps (Cole Parmer) or automated Zoe Organ Chip instruments (Emulate Inc.) in a 37°C cell culture incubator following the manufacturer's instructions at 60ul/hour.

Activation of human LN chip

Chips were treated with cytokines, antibodies, SAC and Fluzone via media perfusion through the top channel. Fluzone (BEI resources, NR-19879, 10ul/ml) or IL4 (Miltenyi Biotec, 130-094-117, 400u/ml) and anti-CD40 antibody (BioXcell, BE0189, 1ug/ml) treatment was initiated 2 days after seeding and SAC treatment was initiated 4 days after seeding (3 days of perfusion). Fresh media was added to the inlet perfusion reservoirs as needed except for Fluzone experiments where reservoirs were maintained as follows: media was recirculated for the first 5 days of treatment i.e. effluents were added back to the inlet perfusion reservoir. At day 5 and

every 3 days thereafter, a 1:1 mix of effluents and fresh media was used for perfusion. This was done to ensure that the cytokine milieu was maintained and to limit and taper the amount of Fluzone consumed by the experiment.

Immunofluorescence Microscopy

To label B and T-cells for microscopy before seeding chips, lymphocytes were labeled with CellTracker dyes (Invitrogen, 1-2μM). LN Chips were fixed by filling the perfusion channel with 4% paraformaldehyde in phosphate-buffered saline (PBS, 1hr at room temperature, RT) and plugging the channel entry and exit ports with 200ul tips containing fixative. Similarly, chips were incubated with primary antibodies diluted in PBS containing 1% FBS and Fc Block (1:20 dilution; Miltenyi Biotec, 130-059-901) overnight at RT, followed by several washes with PBS. Chips were then incubated with secondary antibodies diluted in PBS containing 1% FBS overnight at RT, followed by one-hour incubation with Hoechst (Life Technologies, H3570, 1:1000) and several washes at RT. ECM fibers were imaged using second harmonic imaging after fixation which allows the label-free imaging of biopolymers. Follicles were quantified using the surfaces function on Imaris (BitplanE) software (**Supplementary Fig. 1D)**.

Table 1. List of antibodies used for immunofluorescence microscopy

	Primary Antibody		
Antigen	Supplier	Catalog #	Dilution
CD3	Biolegend	Clone: UCHT1	1:25
CTLA-4	Invitrogen	702534	1:100
AID	Invitrogen	PA5-20012	1:50
CD138	Invitrogen	PA5-47395	1:100

Quantification of T cell polarization

Samples were stained with a fluorophore labeled anti-CD3 antibody (Table 1). Using ImageJ software, random cells were selected, and the center of mass of each cell was defined. Next, the center of mass of the CD3-positive fluorescent region was determined for each cell, and then the absolute distance between the center of the cell and the center of the CD3-stained region was used to define T cell polarization, with greater distances indicating more polarization.

Flow cytometry

Cells were harvested from chips using Cell Recovery Medium (Corning, 354253). Cells were first labeled with Live/Dead fixable dyes (1:1000 dilution; Invitrogen, L34963), followed by a 15 min incubation with fluorophore labeled antibodies and Fc Block (1:100 dilution) at 4°C. Cells were washed twice and then fixed with Cytofix (BD Biosciences, 554655) for 15 minutes at RT. Cells were centrifuged and re-suspended in PBS and stored at 4°C until flow cytometry. Stained Cells were analyzed using LSRFortessa flow analyzer (BD Biosciences). Results were analyzed using FlowJo V10 software (Flowjo, LLC).

Table 2. List of antibodies used for flow cytometry

Antigen	**Supplier**	**Catalog #**	**Per test volume**
CD19	BD Biosciences	340437	10 µL
CD27	BD Biosciences	655429	30µL
IgD	BioLegend	348210	5µL

* A test is defined as a volume of 100ul containing <1 X 10^6 cells. Where possible, the cell number was maintained at 5 X 10^5 cells in 100ul.

Immunoglobulin and Cytokine Quantification

Total immunoglobulin levels were measured using ELISA (Bethyl Biolabs, E80-104 or Mesoscale discovery, K15203D). Influenza HA-specific IgG was detected using a modified

version of a previously described digital ELISA assay (*29*). Briefly, HA from Influenza A/59/Brisbane (BEI Resources, NR-13411) was conjugated to carboxyl-modified paramagnetic beads. Tonsils cultures (2.25-4 X 10^6 cells/well of a 24 well platE) were immunized with 10ul/ml of Fluzone(*40*) were used as positive controls. For detection of anti-HA antibodies, tonsil culture supernatants or chip effluents were incubated with the beads, followed by a biotinylated anti-human Ab [Life Technologies, A18821] and streptavidin-β-galactosidase and analyzed using Simoa HD-1 Analyzer (Quanterix). Tonsils were obtained from Massachusetts General Hospital (MGH) under an Institutional Review Board approved protocol. The digital ELISA was compared to a commercially available ELISA (Abcam, 108745) and found to have much higher sensitivity (**Supplementary Fig. 5**). Similarly, recombinant CXCL13, IFN-g, GM-CSF, IL-10, IL-7 and IL-2 were detected via sandwich digital ELISA using reagents listed in the chart below. Briefly, immune complexes were formed on beads in a 3-step format by 1) capturing target with antibody-conjugated beads, 2) binding with biotinylated detection antibody, and 3) labeling with streptavidin-β-galactosidase. In depth descriptions of Simoa assay development and performance have been previously reported (*29*).

	Protein standard		Capture antibody		Detection antibody	
	Supplier	Catalog #	Supplier	Catalog #	Supplier	Catalog #
IFN-g	R&D Systems	285-IF-100	BioLegend	507502	R&D Systems	MAB285
IL-10		217-IL-005		506801	BioLegend	501501
IL-2		202-IL-010	R&D Systems	MAB602	R&D Systems	MAB202
GM-CSF		215-GM-010		MAB615		BAF215
IL-7		207-IL-005	BioLegend	501302	BioLegend	506601
CXCL13		DY801	R&D Systems	DY801	R&D Systems	DY801

Statistical Analyses

Student's t-tests and tests for linear correlations were performed using Prism (GraphPad SoftwarE). Where distribution of data was not normal, the Mann-Whitney test was used. * indicates $p<0.05$ in all figures.

REFERENCES

1. Seok, J. *et al.* Genomic responses in mouse models poorly mimic human inflammatory diseases. *Proc Natl Acad Sci U A* **110**, 3507–3512 (2013).

2. Eastwood, D. *et al.* Monoclonal antibody TGN1412 trial failure explained by species differences in CD28 expression on CD4+ effector memory T-cells. *Br J Pharmacol* **161**, 512–526 (2010).

3. Tameris, M. D. *et al.* Safety and efficacy of MVA85A, a new tuberculosis vaccine, in infants previously vaccinated with BCG: a randomised, placebo-controlled phase 2b trial. *Lancet* **381**, 1021–1028 (2013).

4. Muramatsu, M. *et al.* Class switch recombination and hypermutation require activation-induced cytidine deaminase (AID), a potential RNA editing enzyme. *Cell* **102**, 553–563 (2000).

5. Mooster, J. L. *et al.* Defective lymphoid organogenesis underlies the immune deficiency caused by a heterozygous S32I mutation in IκBα. **212**, 185–202 (2015).

6. Karrer, U. *et al.* On the key role of secondary lymphoid organs in antiviral immune responses studied in alymphoplastic (aly/aly) and spleenless (Hox11(-)/-) mutant mice. *J. Exp. Med.* **185**, 2157–2170 (1997).

7. Chan, T. D. *et al.* Antigen affinity controls rapid T-dependent antibody production by driving the expansion rather than the differentiation or extrafollicular migration of early plasmablasts. *J Immunol* **183**, 3139–3149 (2009).

8. Paus, D. *et al.* Antigen recognition strength regulates the choice between extrafollicular plasma cell and germinal center B cell differentiation. *J Exp Med* **203**, 1081–1091 (2006).

9. Merville, P. *et al.* Bcl-2+ tonsillar plasma cells are rescued from apoptosis by bone marrow fibroblasts. *J Exp Med* **183**, 227–236 (1996).

10. Grivel, J.-C. & Margolis, L. Use of human tissue explants to study human infectious agents. *Nat Protoc* **4**, 256–269 (2009).

11. Byers, A. M., Tapia, T. M., Sassano, E. R. & Wittman, V. In vitro antibody response to tetanus in the MIMIC system is a representative measure of vaccine immunogenicity. *Biologicals* **37**, 148–151 (2009).

12. Kraus, T. *et al.* Evaluation of a 3D Human Artificial Lymph Node as Test Model for the Assessment of Immunogenicity of Protein Aggregates. *J Pharm Sci* **108**, 2358–2366 (2019).

13. Park, T.-E. *et al.* Hypoxia-enhanced Blood-Brain Barrier Chip recapitulates human barrier function and shuttling of drugs and antibodies. *Nat. Commun.* **10**, 2621 (2019).

14. Musah, S., Dimitrakakis, N., Camacho, D. M., Church, G. M. & Ingber, D. E. Directed differentiation of human induced pluripotent stem cells into mature kidney podocytes and establishment of a Glomerulus Chip. *Nat. Protoc.* **13**, 1662–1685 (2018).

15. Chou, D. B. *et al.* Human bone marrow disorders recapitulated in vitro using organ chip technology. *bioRxiv* 458935 (2018). doi:10.1101/458935

16. Jang, K.-J. *et al.* Liver-Chip: Reproducing Human and Cross-Species Toxicities. *bioRxiv* 631002 (2019). doi:10.1101/631002

17. Cavero, I., Guillon, J.-M. & Holzgrefe, H. H. Human organotypic bioconstructs from organ-on-chip devices for human-predictive biological insights on drug candidates. *Expert Opin. Drug Saf.* **18**, 651–677 (2019).

18. Park, D., Lee, J., Chung, J. J., Jung, Y. & Kim, S. H. Integrating Organs-on-Chips: Multiplexing, Scaling, Vascularization, and Innervation. *Trends Biotechnol.* (2019). doi:10.1016/j.tibtech.2019.06.006

19. Huh, D. *et al.* Reconstituting organ-level lung functions on a chip. *Science* **328**, 1662–1668 (2010).

20. Römer, P. S. *et al.* Preculture of PBMCs at high cell density increases sensitivity of T-cell responses, revealing cytokine release by CD28 superagonist TGN1412. *Blood* **118**, 6772–6782 (2011).

21. Giese, C. *et al.* Immunological substance testing on human lymphatic micro-organoids in vitro. **148**, 38–45 (2010).

22. Angel, M. *et al.* Rho GTPases control migration and polarization of adhesion molecules and cytoskeletal ERM components in T lymphocytes. *Eur. J. Immunol.* **29**, 3609–3620 (1999).

23. Ansel, K. M. *et al.* A chemokine-driven positive feedback loop organizes lymphoid follicles. *Nature* **406**, 309–314 (2000).

24. Havenar-Daughton, C. *et al.* CXCL13 is a plasma biomarker of germinal center activity. *Proc. Natl. Acad. Sci. U. S. A.* **113**, 2702–2707 (2016).

25. Amodio, D. *et al.* Quantitative Multiplexed Imaging Analysis Reveals a Strong Association between Immunogen-Specific B Cell Responses and Tonsillar Germinal Center Immune Dynamics in Children after Influenza Vaccination. *J. Immunol.* **200**, 538–550 (2018).

26. Agematsu, K., Hokibara, S., Nagumo, H. & Komiyama, A. CD27: a memory B-cell marker. *Immunol. Today* **21**, 204–206 (2000).

27. Sanz, I., Wei, C., Lee, F. E.-H. & Anolik, J. Phenotypic and functional heterogeneity of human memory B cells. *Semin. Immunol.* **20**, 67–82 (2008).

28. Opelz, G., Kiuchi, M., Takasugi, M. & Terasaki, P. I. Autologous stimulation of human lymphocyte subpopulation. *J. Exp. Med.* **142**, 1327–1333 (1975).

29. Wu, D., Dinh, T. L., Bausk, B. P. & Walt, D. R. Long-Term Measurements of Human Inflammatory Cytokines Reveal Complex Baseline Variations between Individuals. *Am. J. Pathol.* **187**, 2620–2626 (2017).

30. Arumugakani, G. *et al.* Early Emergence of CD19-Negative Human Antibody-Secreting Cells at the Plasmablast to Plasma Cell Transition. *J. Immunol.* **198**, 4618–4628 (2017).

31. Tesfaye, D. Y., Gudjonsson, A., Bogen, B. & Fossum, E. Targeting Conventional Dendritic Cells to Fine-Tune Antibody Responses. *Front. Immunol.* **10**, (2019).

32. Skelton, J. K., Ortega-Prieto, A. M. & Dorner, M. A Hitchhiker's guide to humanized mice: new pathways to studying viral infections. *Immunology* **154**, 50–61 (2018).

33. Matsuda, Y., Imamura, R. & Takahara, S. Evaluation of Antigen-Specific IgM and IgG Production during an In Vitro Peripheral Blood Mononuclear Cell Culture Assay. *Front. Immunol.* **8**, (2017).

34. Huggins, J. *et al.* CpG DNA activation and plasma-cell differentiation of CD27− naive human B cells. *Blood* **109**, 1611–1619 (2007).

35. Alsughayyir, J., Pettigrew, G. J. & Motallebzadeh, R. Spoiling for a Fight: B Lymphocytes As Initiator and Effector Populations within Tertiary Lymphoid Organs in Autoimmunity and Transplantation. *Front. Immunol.* **8**, (2017).

36. Gu-Trantien, C. *et al.* CXCL13-producing T_{FH} cells link immune suppression and adaptive memory in human breast cancer. *JCI Insight* **2**, (2017).

37. Bovay, E. *et al.* Multiple roles of lymphatic vessels in peripheral lymph node development. *J. Exp. Med.* **215**, 2760–2777 (2018).

38. Díaz-Flores, L. *et al.* Intussusceptive lymphangiogenesis in the sinuses of developing human foetal lymph nodes. *Ann. Anat. - Anat. Anz.* (2019). doi:10.1016/j.aanat.2019.06.004

39. Harding, A. T. & Heaton, N. S. Efforts to Improve the Seasonal Influenza Vaccine. *Vaccines* **6**, (2018).

40. Aljurayyan, A. *et al.* Activation and Induction of Antigen-Specific T Follicular Helper Cells Play a Critical Role in Live-Attenuated Influenza Vaccine-Induced Human Mucosal Anti-influenza Antibody Response. *J. Virol.* **92**, e00114-18 (2018).

ACKNOWLEDGMENTS

General

The authors would like to thank Dr. David Chou for helpful discussions and Dr. Peter Sadow for making surgically removed tonsils available. The following reagents were obtained through BEI Resources, NIAID, NIH: Fluzone® Influenza Virus Vaccine, 2009-2010 Formula, NR-19879 andHA1 Hemagglutinin (HA) Protein with N-Terminal Histidine Tag from Influenza Virus, A/Brisbane/59/2007 (H1N1), Recombinant from Baculovirus, NR-13411 .

Funding

This research was sponsored by funding from the Defense Advanced Research Projects Agency under Cooperative Agreement Number W911NF-12-2-0036 and the Wyss Institute for Biologically Inspired Engineering (to D.E.I.).

Author contributions

G.G. designed all *in vitro* experiments, performed experiments and analysed the data, working with D.E.I, who also supervised all work. P.P, D.C. and J.L. assisted in performing experiments and analysing the data. B.B, L.X. and L.M. designed and conducted all high sensitivity digital ELISAs under the guidance of D.R.W. O.L. and R.P-B. helped with experiment design. G.G, R.P-B. and D.E.I. wrote the manuscript.

Competing Interests

D.E.I. is a founder and holds equity in Emulate, Inc., and chairs its scientific advisory board. G.G. and D.E.I. are co-inventors on a patent application describing the human LN Chip. D.R.W. is a founder and has a financial interest in Quanterix Corporation, a company that develops an ultra-sensitive digital immunoassay platform, and also serves on its Board of Directors. He is an inventor of the Simoa technology.

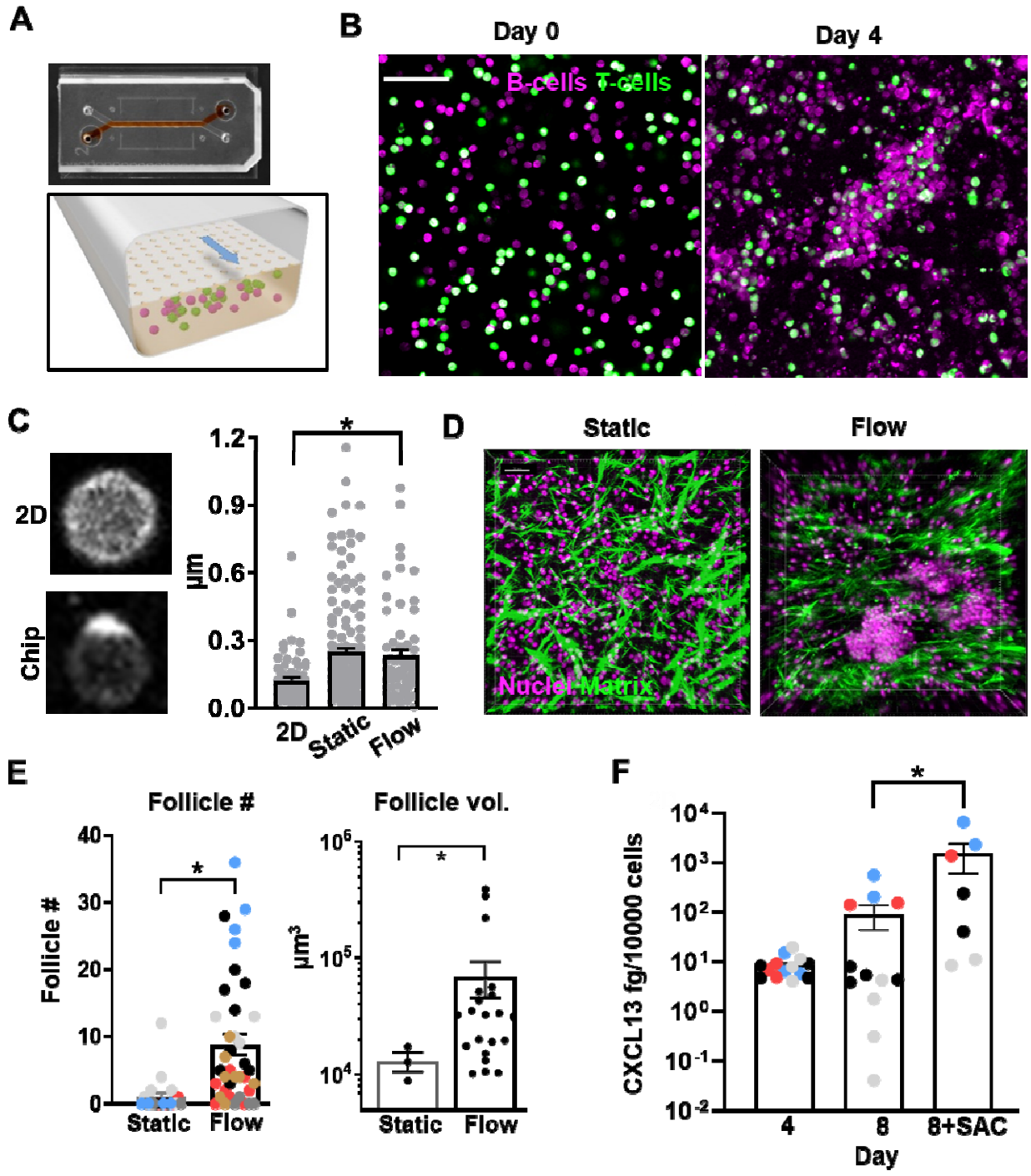

Fig. 1. Perfusion induces LF formation in the human LN chip. **A)** Organ Chip device (top) used for the human LN chip with red dye filling the lower channel and a schematic of the cross section of the device (bottom). **B)** Immunofluorescence micrographs showing CellTracker labeled human B (magentA) and T lymphocytes (green) cultured within an ECM gel in the

device at days 0 and 4 (3 days after perfusion, bar-50 μm). **C)** Immunofluorescence micrographs of T cells in 2D culture versus perfused LN Chip stained for CD3 (left), and quantification of T cell polarization (right). **D)** Second harmonic imaging of ECM fibrils (green) and Hoechst staining of nuclei (magentA) of a static 3D culture vs. perfused 3D culture in the LN Chip (bar, 30μm). **E)** Quantification of LF number (#) and volume (vol.) in cells cultured in static versus perfused (Flow) Organ Chips for 4 days. **F)** CXCL13 levels in effluents of unstimulated LN Chip cultures at 4 and 8 days, and at 8 days when stimulated with SAC on day 4, quantified by high sensitivity digital ELISA. Each colored dot indicates results from a different patient donor (4 donors in total), and * indicates $p<0.05$ in all figures.

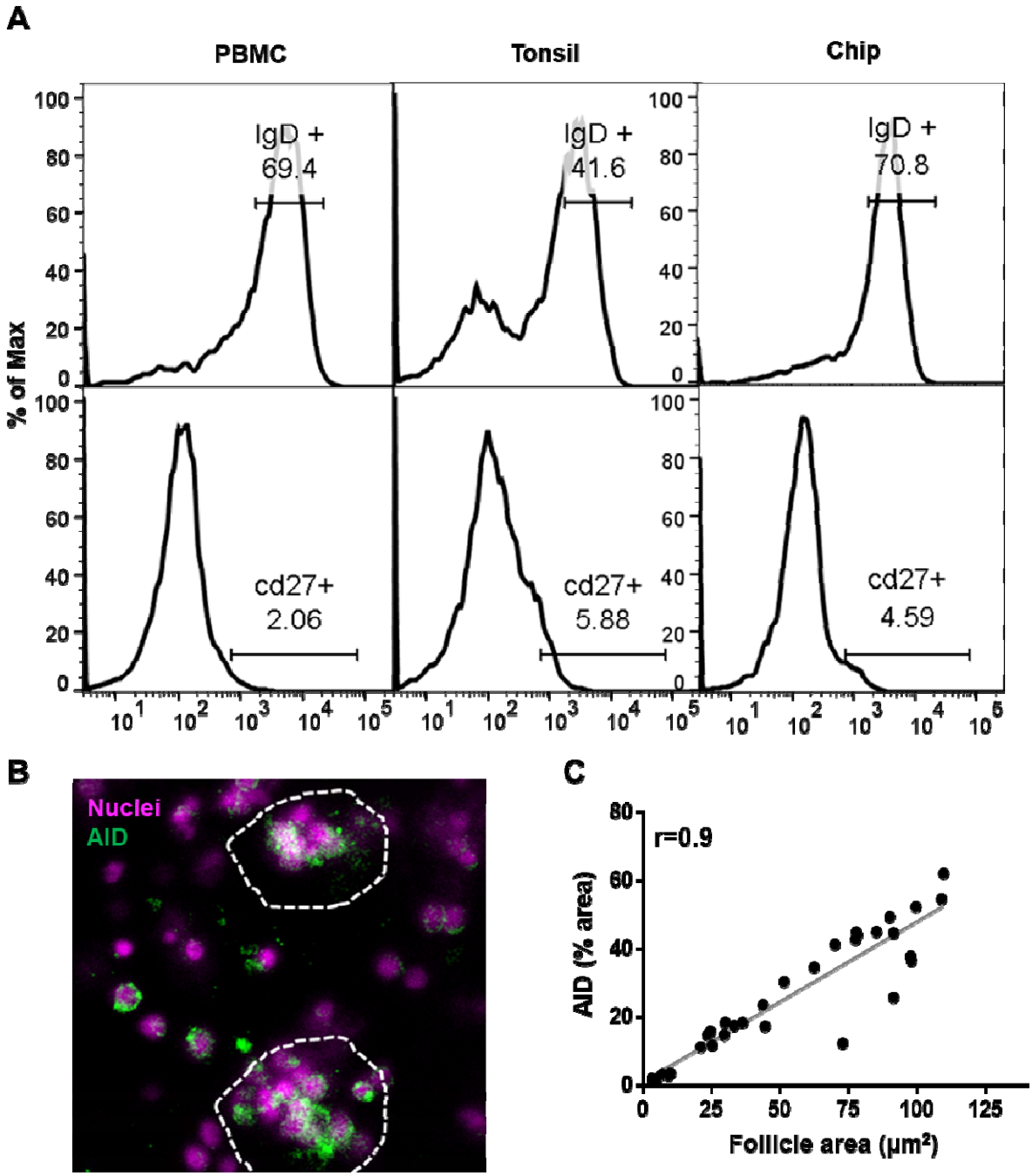

Fig. 2. B cells remain quiescent but express AID in the LFs. **A)** Representative flow cytometric characterization of B cells in the initial PBMC sample (n= 3) compared with cells from explanted tonsils (Tonsil; n = 2) or cells cultured in the LN Chip for 4 days (Chip; n=3). **B)** Representative confocal immunofluorescence micrograph showing AID expression in B cells cultured in the LN Chip for 4 days (similar results were obtained with 4 donors). **C)**

Quantification of AID expression levels in individual follicles as a function of increasing LF area in the LN Chip cultured for 4 days. Each data point represents one follicles and follicles from LN chips from 4 donors were pooled for this analysis.

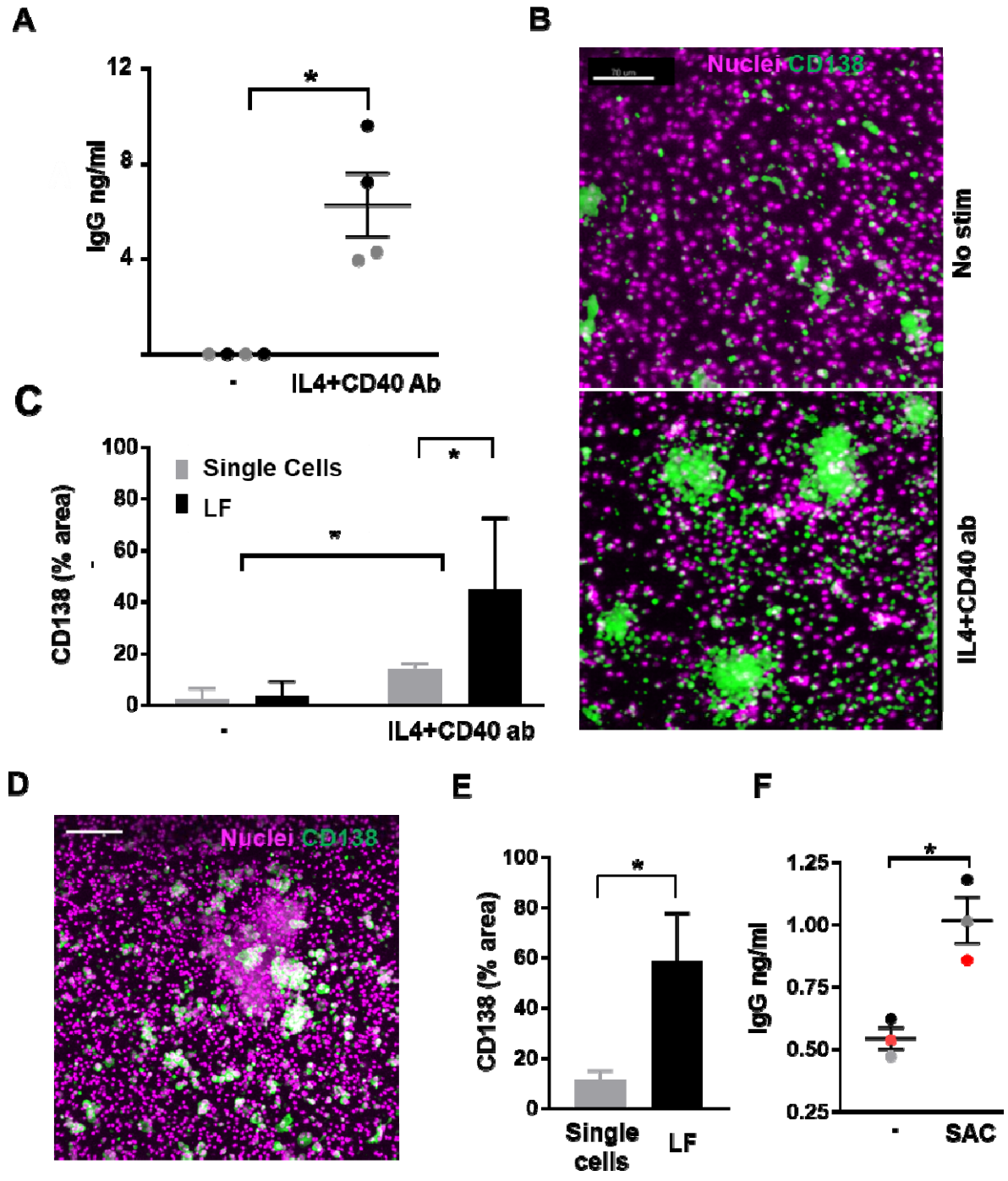

Fig. 3. Class switching and plasma cell formation in the LN chip. A) Total IgG production by the LN chip when engineered with naïve B cells and bulk T cells 6 days after exposure to IL4 and anti-CD40 Ab. Each dot indicates an individual chip from two donors (black and grey). **B)** Immunofluorescence micrographs showing cells in untreated LN chips or chips treated with IL4

and anti-CD40 stained for CD138 (green) and nuclei (magenta; similar results were obtained with cells from 3 donors). **C)** Quantification of CD138 expression in single cells versus cells within LFs within the LN Chip (error bars indicate standard deviation based on analysis of 5 randomly selected fields from 1 donor; similar results obtained in two additional donors). **D)** Immunostaining for CD138 (green) and nuclei (magentA) in SAC-treated chips (similar results obtained with 3 donors, bar 100μm). **E)** Expression of CD138 expression levels measured in isolated cells (Single Cells) versus in follicles (LFs) (results from 5 randomly selected fields from 1 donor; similar results obtained in two additional donors). **F)** Total IgG levels measured in the effluent of the LN chip 3 days after treatment with SAC. Each colored dot indicates results from a different donor.

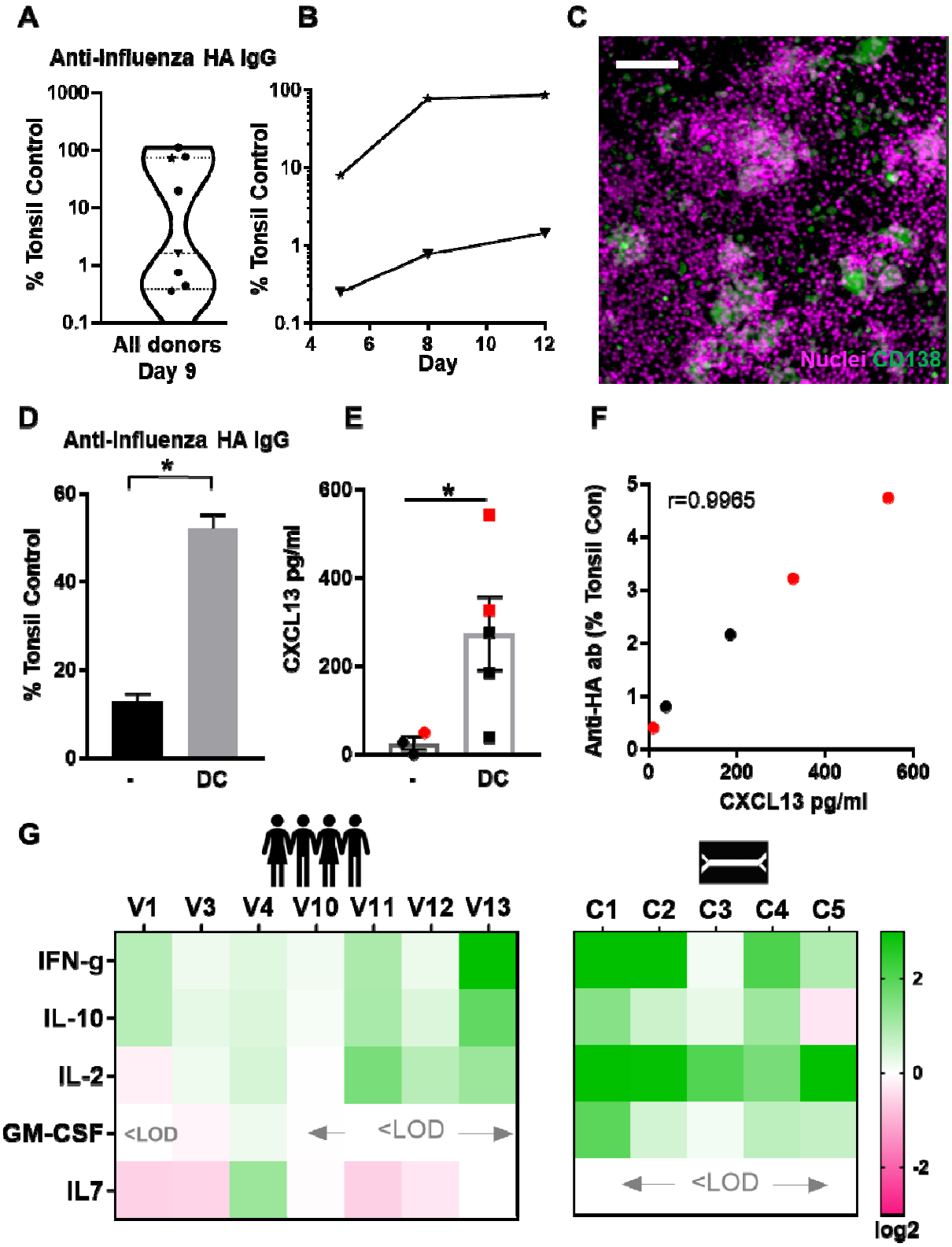

Fig. 4. Influenza vaccination in the human LN chip. A) Anti-HA Ab levels specific to Brisbane/59/H1N1 in effluent of LN Chips, 9 days post-vaccination relative to levels in a culture of tonsillar cells. Each data point represents one donor. **B)** Time course of Ab secretion in representative donors from high (□) and low Ab (▼) groups. **C)** Immunofluorescence micrograph showing CD138 (green) in a Fluzone-stimulated chip (nuclei, magentA) from a high Ab producer (similar results obtained with 3 high Ab producers; bar, 100μm) **D)** Anti-HA Ab levels in effluent of LN Chips with or without DCs, 9 days post-vaccination, relative to levels in a culture of tonsillar cells. One donor shown out of two tested with similar results. **E)** CXCL13 levels in effluent of LN Chips with or without DCs, 5 days post-vaccination. Each colored dot represents an individual chip from two donors (black and reD). **F)** Anti-HA Ab and CXCL13 in effluent of LN Chip 5 days after vaccination. 2 donors shown with each colored dot representing an individual chip. **G)** Fold change (Log_2) in cytokines measured in 7 vaccinated individuals (V1…) or LN Chips from 5 donors (C1-5) compared to pre-vaccination or unvaccinated chips (limit of detection, LOD).